

# Transport of colloids in unsaturated porous media: A pore-scale observation of processes during the dissolution of air-water interface

Sanya Sirivithayapakorn and Arturo Keller

Bren School of Environmental Science and Management, University of California, Santa Barbara  
Santa Barbara, California, USA

Received 15 July 2003; revised 19 September 2003; accepted 1 October 2003; published 5 December 2003.

[1] We present results from pore-scale observations of colloid transport in an unsaturated physical micromodel. The experiments were conducted separately using three different sizes of carboxylate polystyrene latex spheres and Bacteriophage MS2 virus. The main focus was to investigate the pore-scale transport processes of colloids as they interact with the air-water interface (AWI) of trapped air bubbles in unsaturated porous media, as well as the release of colloids during imbibition. The colloids travel through the water phase but are attracted to the AWI by either collision or attractive forces and are accumulated at the AWI almost irreversibly, until the dissolution of the air bubble reduces or eliminates the AWI. Once the air bubbles are near the end of the dissolution process, the colloids can be transported by advective liquid flow, as colloidal clusters. The clusters can then attach to other AWI down-gradient or be trapped in pore throats that would have allowed them to pass through individually. We also observed small air bubbles with attached colloids that traveled through the porous medium during the gas dissolution process. We used Derjaguin-Landau-Verwey-Overbeek (DLVO) theory to help explain the observed results. The strength of the force that holds the colloids at the AWI was estimated, assuming that the capillary force is the major force that holds the colloids at the AWI. Our calculations indicate that the forces that hold the colloids at the AWI are larger than the energy barrier between the colloids. Therefore it is quite likely that the clusters of colloids are formed by the colloids attached at the AWI as they move closer at the end of the bubble dissolution process. Coagulation at the AWI may increase the overall filtration for colloids transported through the vadose zone. Just as important, colloids trapped in the AWI might be quite mobile when the air bubbles are released at the end of the dissolution process, resulting in increased breakthrough. These pore-scale mechanisms are likely to play a significant role in the macroscopic transport of colloids in unsaturated porous media. *INDEX TERMS:* 1831

Hydrology: Groundwater quality; 1832 Hydrology: Groundwater transport; 5139 Physical Properties of Rocks: Transport properties; *KEYWORDS:* air-water interface, DLVO, hydrophobic, colloid, unsaturated, micromodel

**Citation:** Sirivithayapakorn, S., and A. Keller, Transport of colloids in unsaturated porous media: A pore-scale observation of processes during the dissolution of air-water interface, *Water Resour. Res.*, 39(12), 1346, doi:10.1029/2003WR002487, 2003.

## 1. Introduction

[2] Colloid transport in the subsurface has recently attracted significant attention because it can enhance pollutant mobility [McCarthy and Zachara, 1989]. Besides, colloids themselves could be toxic (e.g., radioactive) or pathogenic (e.g., viruses and other microorganisms). When considering drinking water supply contamination, viruses and other microorganisms are usually the main concern [Macler and Merkle, 2000]. In general, viruses as well as other colloids have to move through the vadose zone before they can reach groundwater. Overall, the transport mechanisms of colloids in saturated porous media have been studied in great detail in various aspects [e.g., Small, 1974; Lance and Gerba, 1984; McDowellboyer et al.,

1986; Bales et al., 1989; Corapcioglu and Jiang, 1993; Sim and Chrysikopoulos, 1996; Chrysikopoulos and Sim, 1996; Rehmann et al., 1999; Bradford et al., 2002; Sirivithayapakorn and Keller, 2003]. However, the mechanisms of colloid transport in the unsaturated porous media needed to be understood in greater detail, since there are some significant differences. Transport of colloids in unsaturated porous media has been studied by several researchers at the pore scale, in column experiments and using numerical models [e.g., Powelson et al., 1990; Wan and Wilson, 1994a, 1994b; Poletika et al., 1995; Corapcioglu and Choi, 1996; Sim and Chrysikopoulos, 2000], but there are many issues still unresolved.

[3] In the vadose zone the system contains three phases: air, water, and solid. The principal interaction usually occurs at the solid-water interfaces (SWI) and air-water interfaces (AWI) [Schijven and Hassanizadeh, 2000; Jin and Flury, 2002]. From previous studies, the AWI is usually the

preferred sorption interface for colloids [Powelson *et al.*, 1990; Wan and Wilson, 1994b]. The sorption onto the AWI is strong and considered irreversible [Wan and Wilson, 1994b; Abdel-Fattah and El-Genk, 1998a, 1998b]. However, under strong interfacial shear stresses caused by fast fluid flow, detachment may occur [Wan and Wilson, 1994b; Corapcioglu and Choi, 1996]. The main forces that control particle sorption on the air-water interface are van der Waals, electrostatic, and solvation forces (attractive hydrophobic forces) [Israelachvili, 1992]. In addition, Wan and Wilson [1994b] hypothesized that there are some additional unknown attractive forces when hydrophobic particles are sorbed on the AWI. They hypothesized that those forces could be capillary forces. Sorption onto the AWI increases with increasing particle hydrophobicity, ionic strength in the solution, and decreasing moisture content and could be limited by the capacity of the interface and the accessibility of the interface to the particles in the solution [Lance and Gerba, 1984; Wan and Wilson, 1994b; Abdel-Fattah and El-Genk, 1998a]. Wan and Wilson [1994a] also showed that AWI movement during drainage, imbibition, or a bubbling process could increase the movement of the colloids down to the deeper vadose zone.

[4] In several mathematical models developed to simulate colloid transport in porous media, the sorption of colloids on to the AWI was assumed irreversible and dependent on moisture content [e.g., Yates and Ouyang, 1992; Corapcioglu and Choi, 1996; Sim and Chrysikopoulos, 2000]. In a mathematical model developed by Corapcioglu and Choi [1996], the mass transfer of colloids to the AWI was formulated as a second-order kinetics process, assuming no desorption. They found that the total colloidal capture to the AWI is affected by the rate of colloid capture as well as the available fraction of AWI. The model was also used to simulate transient flow conditions with variable saturations, such as during filtration. For this simulation the hydrodynamic dispersion coefficient and the colloidal sorption capacity of the AWI were functions of pore water velocity and air saturation, respectively, and were calculated as the wetting front moves. Both experimental data and model results show that the presence of AWI significantly retards colloid transport. In the experiments, most of the colloid particles were held at the AWI, while the wetting front progresses along the column. In the numerical study by Sim and Chrysikopoulos [2000], the model simulation indicated that virus sorption is greater at the AWI than liquid solid interface.

[5] The mathematical model developed by Sim and Chrysikopoulos [2000] for virus transport in a one-dimensional, homogeneous, unsaturated porous medium is as follows:

$$\frac{\partial}{\partial t}[\theta_m C] + \rho \frac{\partial C^*}{\partial t} + \frac{\partial}{\partial t}[\theta_m C^\infty] = \frac{\partial}{\partial z} \left[ D_z \theta_m \frac{\partial C}{\partial z} \right] - \frac{\partial}{\partial z} [qC] - \lambda \theta_m C - \lambda^* \rho C^* - \lambda^\circ \rho C^\infty \quad (1)$$

[6] Under unsaturated conditions, the accumulation of particles at the solid-liquid and air-liquid interfaces was hypothesized to be described by the following expressions [Sim and Chrysikopoulos, 1999, 2000]:

$$\rho \frac{\partial C^*}{\partial t} = k \theta_m [C - C_g] - \lambda^* \rho C^* \quad (2)$$

$$\frac{\partial \theta_m C^\infty}{\partial t} = k^\circ \theta_m C - \lambda^\circ \theta_m C^\infty \quad (3)$$

where is  $C(t, z)$  the liquid phase concentration of colloids [ $M L^{-3}$ ];  $C^*(t, z)$  is the adsorbed colloid concentration at the liquid-solids interface [ $M M^{-3}$ ];  $C^\infty(t, z)$  is the adsorbed colloid concentration at the air-liquid interface [ $M L^{-3}$ ];  $C_g(t, z)$  is the liquid phase concentration of colloids in direct contact with solids [ $M L^{-3}$ ] which is assumed to be equal to  $C^*/k_a$ ;  $q$  is the specific discharge (Darcian fluid flux) [ $L t^{-1}$ ];  $\theta_m$  is the moisture content (moisture volume divided by the total volume of the porous media);  $\rho$  is the bulk density of the solid matrix [ $M L^{-3}$ ];  $\lambda^*$  is the transformation rate coefficient of colloids sorbed at the liquid-solid interface [ $t^{-1}$ ] (e.g., virus inactivation rate when sorbed onto solids);  $\lambda^\circ$  is the transformation rate coefficient of colloids sorbed at the AWI [ $t^{-1}$ ];  $k$  is liquid to liquid-solid interface mass transfer rate [ $t^{-1}$ ];  $k^\circ$  is liquid to air-liquid interface mass transfer rate [ $t^{-1}$ ];  $t$  is time [ $t$ ];  $z$  is a spatial coordinate increasing in the downward direction [ $L$ ]; and  $D_z$  is vertical hydrodynamic dispersion coefficient [ $L^2 t^{-1}$ ]. Sim and Chrysikopoulos [2000] described the sorption of colloids onto solid-liquid interfaces as a reversible process (equation (2)), while the sorption of colloids onto liquid-air interfaces was described as an irreversible process (equation (3)).

[7] Thus, under unsaturated conditions, colloids were hypothesized to remain irreversibly sorbed at the air-liquid interface due to capillary forces [Wan *et al.*, 1994; Sim and Chrysikopoulos, 2000]. In the transition to a saturated system, we hypothesize that sorption at the AWI becomes reversible as the interface decreases. From our previous experiments with saturated and unsaturated micromodels [Keller *et al.*, 1997; Sirivithayapakorn and Keller, 2003], we observed how air bubbles trapped in the pore spaces undergo dissolution as water imbibe into a dry micromodel. We determined that micromodels could be used as an analog for colloid transport processes in the vadose zone, for example, following rainfall infiltration, irrigation, a septic tank leak, or a discharge event. Using the micromodels, we sought to observe desorption of colloids from the AWI during the dissolution of air bubbles.

[8] In this study we investigated the transport process of colloids during the dissolution of the air bubble. We demonstrated how the colloids could mobilize during the infiltration of surface water through the vadose zone. The experiments were set up to investigate, at the pore scale, the mechanisms of transport of three different sizes of carboxylate polystyrene latex spheres and Bacteriophage MS2 virus under unsaturated conditions at different water content levels.

## 2. Methods

### 2.1. Experimental Setup

[9] The present experiments were conducted at the pore scale using physical micromodels, based on the experimental setup that has been previously developed and applied by Keller *et al.* [1997] (Figure 1). The physical micromodels used in this study contain a repeated realistic pattern of pore networks with pore diameters ranging from 2.4 to 30  $\mu m$  (Figure 2). The porosity of the micromodel used here has been experimentally determined to be 37%. The surface of

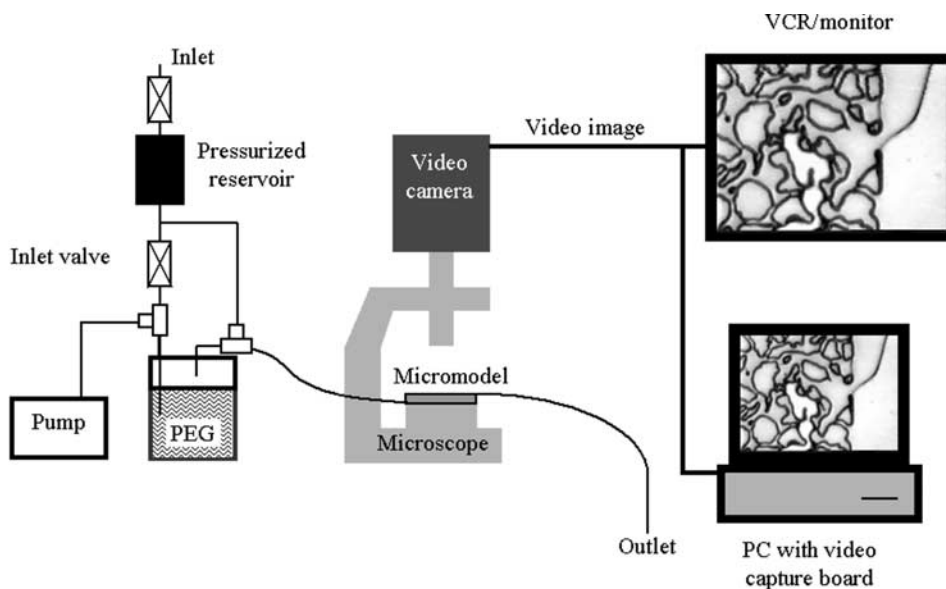


**Figure 1.** Experimental setup. Moist air created by passing air through the PEG solution to create and unsaturated condition in the micromodel.

the pore network was made of silicon that has been oxidized after etching, leaving a water-wetting surface, approximately  $15\ \mu\text{m}$  deep. The etched silicon wafer was then placed between two glass plates. The top glass plate was attached to the silicon wafer using anodic bonding.

[10] Ports were constructed on the top plate to allow independent injection and extraction from different directions. To ensure that the model remains water-wet, carbon dioxide was introduced to displace the air, and then water was injected, which eventually dissolves the carbon dioxide, allowing the wetting fluid to saturate the model completely. This was typically followed by injection of a 10% acetic acid solution into the micromodel for at least 50 pore volumes to produce a hydrophilic surface, similar to most natural clay and sand surfaces [Keller *et al.*, 1997]. The acetic acid was flushed out with dilute-buffered millipore water for at least 100 pore volumes. The dilute-buffered millipore water was used as medium for all experiments. This solution contained  $0.012\ \text{mM}$  of  $\text{Na}_2\text{HPO}_4$  and  $0.010\ \text{mM}$  of  $\text{KH}_2\text{PO}_4$ . The ionic strength of the solution was determined to be  $0.04\ \text{mM}$ . In all cases, the model was strongly water-wet in the presence of air as observed from the contact angle of water and air with the micromodel [Keller *et al.*, 1997]. The main component of the surface of the micromodel was silica and silicon hydroxides [Keller *et al.*, 1997]. The wetted surface in the micromodel was covered with surface hydroxyl groups; this surface is generally negatively charged at neutral pH [Wan and Wilson, 1994b].

[11] An industrial microscope (Nikon Optiphot-M) was used to image the micromodel pore space. Epifluorescence microscopy was used to view the fluids and colloids in the pore space. The images were captured with a charge-coupled device (CCD) camera (Sanyo VDC-2972) at a high resolution ( $1/2$ -inch CCD color image sensor, 470 line horizontal resolution). A video frame grabber (Integral Technologies Flashpoint) was used to acquire the image by the computer. A digital camera (Sony Digital Handycam) was also connected to the CCD TV system to acquire a

video stream of real-time movement of colloid. Flow rate was measured at the inlet, using digital flowmeters (Fischer Scientific Model 1000).

[12] The colloids used in this study were carboxylate polystyrene latex spheres (Sigma-Aldrich), with mean diameter of  $3.0$ ,  $2.0$ ,  $1.0$ , and  $0.05\ \mu\text{m}$  and freeze-dried Bacteriophage MS2 (ATTC). The Bacteriophage MS2 was stained with cyanine-based nucleic acid stain, Yo-Pro-1 {4- [3-methyl-2, 3-dihydro- (benzo-1, 3-oxazole)-2-methyl-methylidene] - 1 - (3'-trimethyl ammoniumpropyl)-quinolinium diiodide} (Molecular Probes). A vial (approximately  $1\ \text{mL}$ ) of freeze-dried Bacteriophage MS2 was rehydrated in  $500\ \text{mL}$  millipore water before the staining process. The staining procedure followed the approach used by Hennes *et*

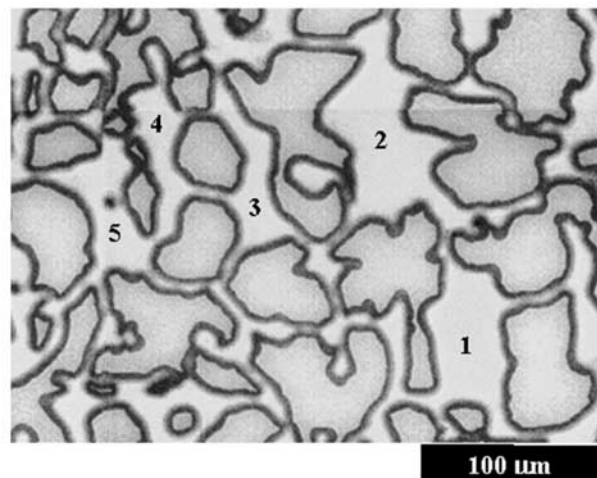


**Figure 2.** Composite image of a section of the etched pattern in the micromodel. Pore spaces are labeled from 1 to 5. See Sirivithayapakorn and Keller [2003] for the complete pattern.

al. [1995]. After the staining process, the filter papers that contained the stained Bacteriophage were washed with millipore water to collect the stained particles. The stained particles were later injected into the micromodel.

[13] For each colloidal suspension, including MS2, we prepared three 1-mL samples. To measure the colloid concentration, each sample was gently filtered on a 0.02  $\mu\text{m}$  pore size  $\text{Al}_2\text{O}_3$  Anodisc 25 mm membrane filter (Whatman) along with 0.45  $\mu\text{m}$  pore size cellulose nitrate as a backing filter. A direct count method was used to quantify the concentration of colloids and MS2, following *Hennes et al.* [1995]. The concentrations of colloid suspension were calculated in the range of  $10^3$ – $10^4$  particles per milliliter.

[14] Solutions of polyethylene glycol M.W. 8000 (PEG) were prepared with a concentration of 100 g/L, to generate a controlled moisture air phase flow into the micromodel [Holden, 2001], producing a moist but unsaturated condition in the initially dry micromodel (Figure 1). The water content in the micromodel was calculated by comparing the images of the dry and wet model, using image analysis software (Scion Image). The available air-liquid interface was quantified by measuring it directly from the selected field of view of  $600 \times 600 \mu\text{m}$ . From these experiments, we found that the setup and the technique of image analysis used here can accurately quantify the water content in the selected field of view if it is more than about 10%; below a water content of 10%, the uncertainty in moisture content measurement increases significantly, since water is mostly in thin films and crevices at that point. The available AWI was also measured from the images. No surfactant was added to stabilize the trapped air bubble.

[15] After passing the moist air through the micromodel for 2 days, the moist air was stopped and water with suspended colloids was introduced into the micromodel at a very low flow rate (i.e., with a pressure gradient of less than 1 kPa). Once there were about four to five colloid particles sorbed onto the air-liquid interfaces we were observing, a dilute buffer solution without colloid particles was introduced into the micromodel at the same low-pressure gradient. The buffer solution consisted of  $\text{K}^+$  0.005,  $\text{Na}^+$  0.024,  $\text{H}_2\text{PO}_4^-$  0.005, and  $\text{HPO}_4^{2-}$  0.012 mM. The water flow rate was then increased to start the dissolution process of the trapped air bubbles. The pressure on the dilute buffer solution was 133 kPa, resulting in a water flow rate through the micromodel of about  $3.2 \text{ cm}^3 \text{ d}^{-1}$ , which correspond to average water velocity of  $0.9 \text{ m d}^{-1}$ . Time series of all the dissolution and colloid release events were captured using the microscope's CCD camera.

[16] The images and video streams were taken from selected regions in the micromodel, which include various pore bodies and pore throat sizes. From the repeat pattern in the micromodel, five pore spaces were selected (Figure 2). The experiments were planned to observe the behavior of colloids when the water content changes. Each pore was observed five times.

## 2.2. Calculation of the Interaction Energy

[17] The interaction between the colloids and AWI at the observed scale depends on forces that act at a short distance. To better understand the behavior of the colloids and the AWI, we calculated the interaction energy  $W$  of both colloid-colloid and colloid-AWI using the Derjaguin-Landau-Verwey-Overbeek (DLVO) theory of colloid

stability [Israelachvili, 1992]. For colloid-colloid interaction in water,  $W$  is calculated based on the sum of electrostatic double layer repulsion,  $V$ , and van der Waals attraction forces,  $A_{vdW}$ , as follows:

$$W = V + A_{vdW} = 2\pi r \epsilon \epsilon_0 \psi_0^2 \exp(-\kappa D) - \frac{Ar}{12D} \quad (4)$$

where  $r$  is the radius of the colloids (m),  $\epsilon$  is the dielectric constant of water,  $\epsilon_0$  is the permittivity in free space ( $\text{C}^2 \text{ J}^{-1} \text{ m}^{-1}$ ),  $\psi_0$  is the colloid surface potential (V),  $\kappa$  is the inverse Debye length ( $\text{m}^{-1}$ ),  $D$  is the minimum separation distance (m), and  $A$  is the Hamaker constant for colloid interacting across water (J).

[18] The inverse Debye length was calculated from the following equation [Shaw, 1992; Israelachvili, 1992].

$$\kappa = \left( \sum_i \frac{2\rho_{\infty,i} e^2 z_i^2}{\epsilon \epsilon_0 kT} \right)^{1/2} = \left( \sum_i \frac{2N_A C_i e^2 z_i^2}{\epsilon \epsilon_0 kT} \right)^{1/2} \quad (5)$$

where  $\rho_{\infty,i}$  is the ion density of species  $i$  in the bulk solution ( $\text{m}^{-3}$ ),  $N_A$  is Avogadro's number ( $\text{mol}^{-1}$ ),  $C_i$  is the concentration of specie  $i$  ( $\text{mol m}^{-3}$ ),  $e$  is the electronic charge (C),  $z_i$  is the valency of species  $i$ ,  $k$  is Boltzmann's constant ( $\text{J K}^{-1}$ ), and  $T$  is the absolute temperature (K).

[19] The value of  $A$  for the interaction of polystyrene spheres across water was obtained from Parsegian [1981], while the value of  $A$  for the interactions of MS2 capsid across water and for either latex sphere or MS2 and air bubble across water were calculated from the following equation according to the Lifshitz theory [Israelachvili, 1992]:

$$A = \frac{3}{4} kT \left( \frac{\epsilon_1 - \epsilon}{\epsilon_1 + \epsilon} \right) \left( \frac{\epsilon_2 - \epsilon}{\epsilon_2 + \epsilon} \right) + \frac{3h\nu_e}{8\sqrt{2}} \frac{(n_1^2 - n^2)(n_2^2 - n^2)}{(n_1^2 + n^2)^{1/2} (n_2^2 + n^2)^{1/2} \left\{ (n_1^2 + n^2)^{1/2} + (n_2^2 + n^2)^{1/2} \right\}} \quad (6)$$

where  $h$  is Planck's constant (J-s),  $\nu_e$  is absorption frequency ( $\text{s}^{-1}$ ),  $\epsilon_1$  is dielectric constant of colloids,  $\epsilon_2$  is dielectric constant of air,  $n_1$  is refractive index of colloid,  $n_2$  is refractive index of water, and  $n$  is refractive index of water. In case of interaction of MS2 capsid across water,  $\epsilon_1$  is equal to  $\epsilon_2$  and  $n_1$  is equal to  $n_2$ .

[20] For the interaction energy between the trapped air bubble and colloids, the double layer repulsion  $V$  was calculated based on expression presented by Gregory [1975], assuming constant charge and linear-superposition as follows:

$$V = \left( \sum_i N_A C_i \right) \frac{128\pi kT}{\kappa^2} \gamma_1 \gamma_2 \frac{rR}{(r+R+D)} \exp(-\kappa D) \quad (7)$$

$$\gamma_j = \tanh\left(\frac{y_j}{4}\right), \quad j = \text{either 1 or 2} \quad (8)$$

where  $R$  is the average radius of trapped air bubble before the dissolution process and  $y_j$  is the reduced potential at any

**Table 1.** Values of Parameters Used in the Calculation of Interaction Energy

Parameter	Value	Note
Radius of MS2, $r$ , m	$1.25 \times 10^{-8}$	
Average radius of trapped air bubble before the dissolution process, $R$ , m	$5 \times 10^{-5}$	this study
Dielectric constant $\epsilon$		
Water	78	
Virus capsid	4.00	<i>Reddy et al.</i> [1998]
Latex sphere	2.50	manufacturer, Sigma
Permittivity in free space $\epsilon_0$ , $C^2 J^{-1} m^{-1}$	$8.85 \times 10^{-12}$	
Surface potential $\psi_0$ , V		
Carboxylate polystyrene latex	-0.053	<i>Wan and Wilson</i> [1994a]
MS2	-0.020	<i>Penrod et al.</i> [1996]
Hamaker constant $A$ , J		
Polystyrene interacting across water	$1.37 \times 10^{-20}$	<i>Parsegian</i> [1981]
MS2 interact across water	$3.12 \times 10^{-20}$	calculated from equation (3)
Avogadro's number $N_A$ , $mol^{-1}$	$6.022 \times 10^{23}$	
Electronic charge $e$ , C	$-1.602 \times 10^{-19}$	
Boltzmann's constant $k$ , $J K^{-1}$	$1.381 \times 10^{-23}$	
Absolute temperature $T$ , K	298	
Planck's constant $h$ , $J s^{-1}$	$6.626 \times 10^{-34}$	
Absorption frequency for water $\nu_w$ , $s^{-1}$	$3.0 \times 10^{15}$	<i>Israelachvili</i> [1992]
Refractive index $n$		
Water	1.33	
MS2	1.06	<i>Balch et al.</i> [2000]
Latex sphere	1.51	manufacturer, Sigma

distance from the surface of 1 and 2, or in this case colloids and air bubbles, and was calculated by the following expression:

$$y_j = \frac{\Psi}{kT} \left( \sum_i z_i e \right) \quad (9)$$

The values of parameters used in the above calculations are given in Table 1.

### 3. Results and Discussion

[21] The average initial water content of the micromodel was 15% (varying from 11% to 22%). The results from all visual observations are very similar regardless of particle size; therefore we present examples of dissolution sequences for 1  $\mu m$  latex colloid and MS2 at the AWI in the set of images presented in Figures 3 and 4, respectively. In both cases, the dissolution of the AWI was slow at the beginning and accelerated toward the end of the dissolution process, as more gas phase surface area (AWI) became available for mass transfer of gas molecules relative to the volume of trapped air. The particles were initially transported by advective liquid flow, with little diffusion across streamlines, given the particle size. There was significant dispersion at larger scales as observed in previous studies [e.g., *Sirivithayapakorn and Keller*, 2003]. As the particles moved closer to the AWI, they slowed down due to the restricted flow around the air bubble. The colloids migrated to the vicinity of the AWI via advective flow in the streamlines near the bubble or by diffusion. Once the colloids were near the AWI, they were attracted by attractive interactions or through direct collision, and finally attached to the AWI.

[22] Figure 3a starts the sequence with a cluster of colloids attached to the AWI. Additional individual colloids continue to flow by. All of the colloids observed in this

sequence become trapped at the same AWI (Figure 3b). We did not observe any individual colloid detachment from the AWI, and we did not observe any colloid attachment to or detachment from the SWI. As dissolution of the air bubble progresses, colloids attached to the AWI are brought closer and may adhere to each other (Figures 3b–3f). Clustering probably occurs when the attached colloids reach the range of primary minimum according to DLVO theory, since the colloids in the cluster do not redisperse in the solution. When the air dissolution process is advanced, the cluster of colloids is transported by the advective flux, as the bubble disappears (Figures 3e–3f).

[23] For MS2 at the AWI (Figure 4), the dissolution sequence of air bubble is similar to that when latex colloids are present at the AWI. In Figure 4 the sequence starts with about six discrete MS2 particles attached to the AWI. Similar to the latex particles in Figure 3, the MS2 viruses are brought together as the air bubble dissolves, and finally form a cluster and move away with the flow (Figures 4a–4f).

[24] Generally, there was no desorption of individual latex colloids or Bacteriophage MS2 from the AWI observed before and during air bubble dissolution. During the dissolution, two mechanisms were observed that can mobilize the colloids. First, if the trapped air bubble is dislodged, as the dissolution process advances and it is no longer held within the pore space, the colloids will move along with the air bubble, trapped at the AWI. Second, only when the dissolution process is very advanced can the colloids trapped at the AWI form a cluster that detaches and moves along with the flow (Figures 3f and 4e). The colloids around the AWI typically will form only one cluster. Once released, the clusters can attach down-gradient to other air bubbles that have not been dissolved (e.g., Figure 3a). A large cluster may obstruct the flow down-gradient, as it becomes trapped in a pore throat. In fact, a number of our initial experiments had to be repeated due to pore clogging.

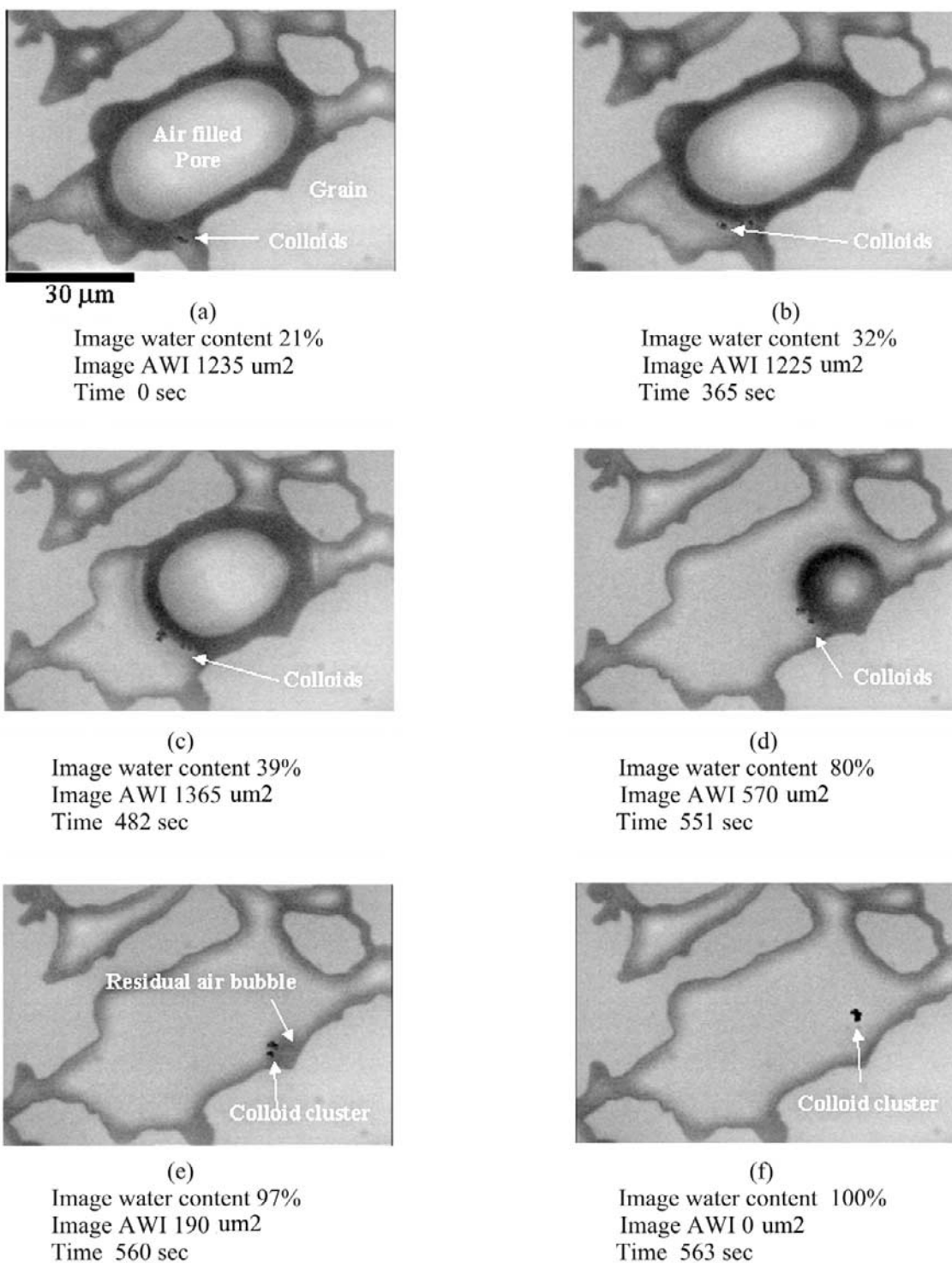


**Figure 3.** Air bubble dissolution time series at 133 kPa, with 1 mm latex colloids at the air-water interface (AWI), under  $\times 500$  fluorescence microscope. The AWI in the image (image AWI) is calculated based only on the surface of AWI that is in contact with flowing water.

[25] The calculation results for the interaction energy between these colloids, according to the DLVO theory, are given in Figure 5. For the interaction between the colloids used in our experiments, the DLVO forces should be sufficient to describe the interaction of the colloids due

mainly to the nature of the surfaces and the size of the colloids [Israelachvili, 1992]. The results suggest that colloids in solution are in a metastable state, in which the separated particles are at a lower energy than the aggregate. Repulsion forces dominate; therefore the system is kineti-

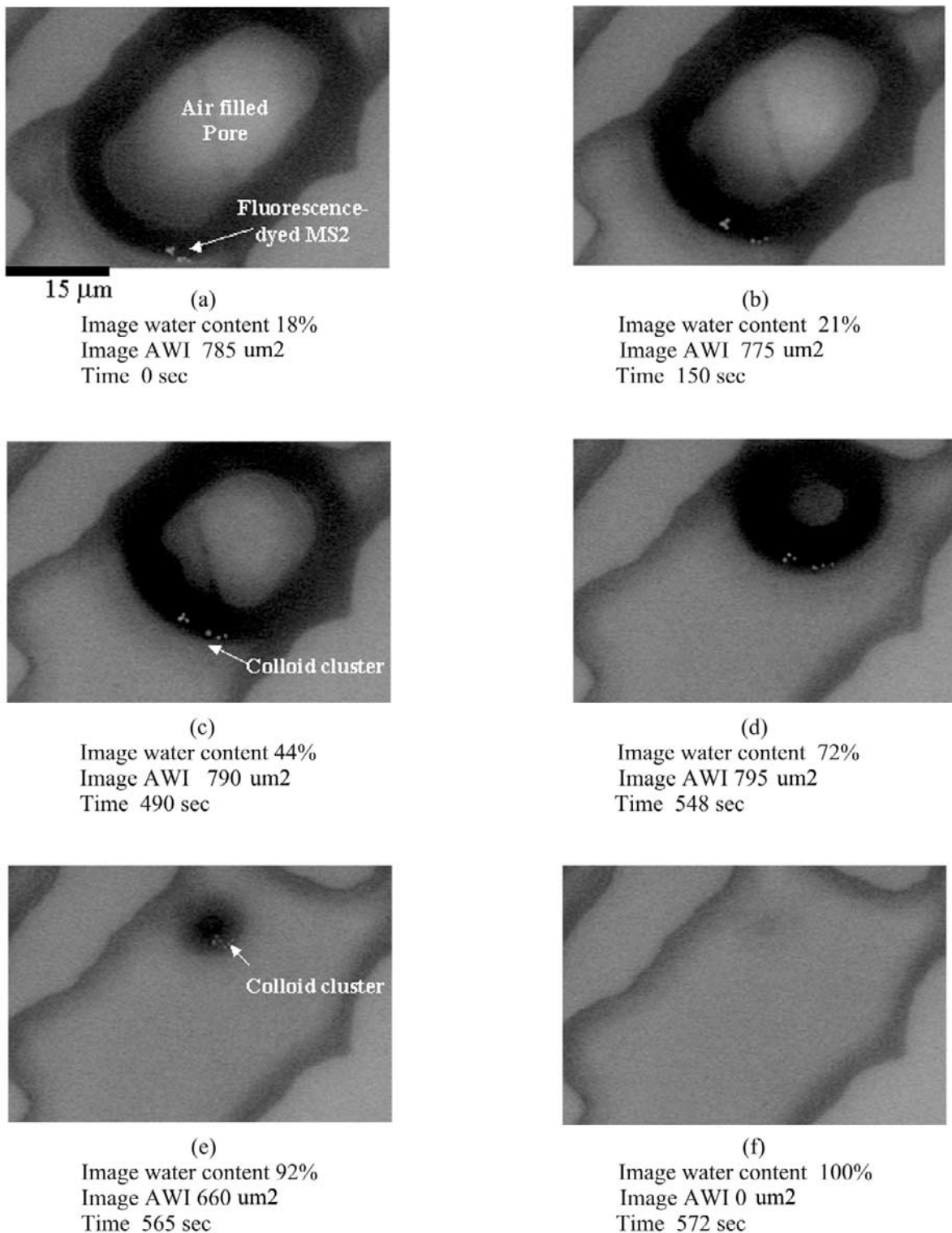


**Figure 4.** Air bubble dissolution time series at 133 kPa, with fluorescence-dyed Bacteriophage MS2 at the air-water interface (AWI), under  $\times 1000$  fluorescence microscope. The AWI in the image (image AWI) is calculated based only on the surface of AWI that is in contact with flowing water.

cally stable [Hiemenz and Rajagopalan, 1997]. The energy barriers for these colloids are about 3300, 2100, 1000, 54, and 3 kT for 3, 2, 1, and 0.05  $\mu\text{m}$  polystyrene and MS2, respectively (Figures 5a and 5b), which are in the range of

typical DLVO forces and much smaller compared with a hydrogen bond [Israelachvili, 1992]. Considering the calculated energy barriers, the 0.05  $\mu\text{m}$  latex colloids and MS2 will coagulate at a faster rate compared with the other

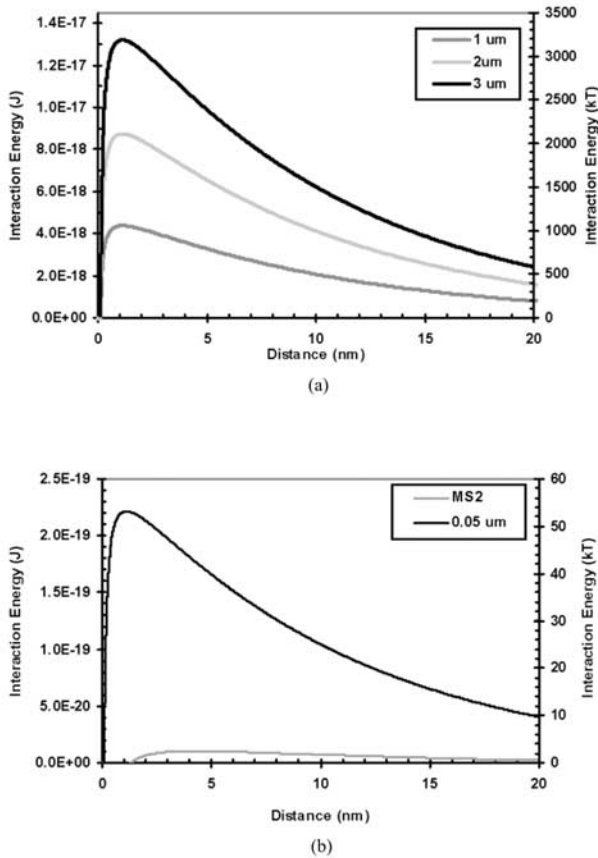


**Figure 5.** Calculated interaction energy according to the DLVO theory between two colloidal particles based on the condition described in this experiments and the parameters given in Table 1 for (a) 1, 2, and 3  $\mu\text{m}$  colloids and (b) 0.05  $\mu\text{m}$  colloid and MS2.

colloids because of their low energy barriers. Nevertheless, we did not observe immediate coagulation of colloids either in the suspension or when trapped at the AWI. The DLVO calculations suggest that the clusters of colloids observed at the AWI before dissolution or at the beginning of the dissolution process are the result of released upstream clusters that are transported downstream, rather than immediate coagulation at the AWI. This is probably particularly the case for larger colloids (2 and 3  $\mu\text{m}$ ). The upstream clusters are formed at the end of the dissolution process of the bubbles upstream.

[26] For an asymmetric system, e.g., a system of dissimilar surfaces, such as the surface of colloids and AWI of bubbles in this case, the van der Waals and double layer forces may be attractive or repulsive [Israelachvili, 1992]. Therefore the net DLVO forces may be attractive or repulsive, or the sign and gradient may vary in a complex way as a function of distance [Ducker et al., 1994]. Given that the dielectric constant and the refractive index of air are equal to 1, the calculated Hamaker constant for all sizes of latex colloids interacting with the AWI across water according to equation (6) is negative ( $-3.50 \times 10^{-20}$  J). Thus the van der Waals interaction would be repulsive. However, the Hamaker constant calculated for MS2 under the same conditions is positive ( $6.10 \times 10^{-20}$  J). Given the size of

the trapped air bubbles in our system, about 50  $\mu\text{m}$  in diameter, the surface potential of the air bubble should be in the range of  $-100$  mV [Usui et al., 1981], which is larger than both the surface potential of latex colloids or MS2 (Table 1). After calculating the double-layer interaction energy between colloids or MS2 and the AWI using equations (7)–(9), and combining it with the van der Waals interaction energy, the resulting interaction is repulsive at all separation distances. Thus, according to DLVO theory, it would not be likely to observe colloids readily attaching to the AWI, since attachment is not favorable. It should be noted that according to the calculation presented by *Abdel-Fattah and El-Genk* [1998b], the interaction energy between colloids and the AWI is not necessarily repulsive at all separation distances, but there might be a significant energy barrier to overcome. Given that our solution has very low ionic strength, 0.04 mM, the energy barrier could be at least of the order of  $10^3$  kT for all colloids.

[27] However, as observed here, as well as by *Wan and Wilson* [1994b], the polystyrene latex colloids and MS2 attach strongly to the AWI; the forces accounted for in the DLVO theory alone cannot explain this phenomenon. The strong attraction between these particles and the AWI may be explained by additional non-DLVO forces, i.e., hydrophobic forces, which operate at a longer range and are much stronger than the van der Waals and double layer forces [Israelachvili, 1992]. For example, for the interaction between hydrophilic silica particles and air bubbles, the attraction energy has been estimated to be as high as 0.2 mJ [Ducker et al., 1994], which is several orders of magnitude higher than common van der Waals and double layer interaction energies calculated by us in the previous paragraphs. Therefore it is quite possible that hydrophobic forces control colloid attachment to the AWI.

[28] It has been theorized that the attached particles could penetrate the bubble surface after contacting the AWI and may adhere to the surface of the bubble by capillary forces [Tchaliyovska et al., 1990; Ducker et al., 1994; Wan and Wilson, 1994b]. A detailed explanation of these processes is given by *Ducker et al.* [1994]. The necessary capillary energy  $W_0$  can be calculated from

$$W_0 = \gamma(1 - \cos \theta) \quad (10)$$

where  $\gamma$  is the surface tension of water,  $72.8 \text{ mJ m}^{-2}$ , and  $\theta$  is the contact angle, in degrees [Ducker et al., 1994]. The contact angle of a latex particle with water is about  $36^\circ$  [Wan and Wilson, 1994a]. For MS2, the contact angle is about  $40^\circ$ , estimated from the contact angle of bacteria that have high peptide concentration at the cell wall for the value of contact angle for MS2 [Dufrene et al., 1997]. The calculated capillary energy across the AWI, assuming an equilibrium contact angle of  $36^\circ$  for latex colloids and  $40^\circ$  for MS2, would be of the order of 14 and 17  $\text{mJ m}^{-2}$  for the latex colloids and MS2, respectively.

[29] On the basis of these calculations, a colloidal particle held by capillary forces at the point of contact with the AWI will penetrate the AWI. The penetration distance  $D_0$  can be estimated according to *Ducker et al.* [1994] as follows:

$$D_0 = R(1 - \cos \theta) \quad (11)$$

**Table 2.** Calculated Capillary Energy  $W_{\text{cap}}$ 

Colloid	$D_0$ , m	$W_{\text{cap}}$ , J	$W_{\text{cap}}$ , kT
Latex sphere 3 $\mu\text{m}$	$2.8 \times 10^{-7}$	$3.4 \times 10^{-14}$	$8.3 \times 10^6$
Latex sphere 2 $\mu\text{m}$	$1.9 \times 10^{-7}$	$1.5 \times 10^{-14}$	$3.7 \times 10^6$
Latex sphere 1 $\mu\text{m}$	$9.5 \times 10^{-8}$	$3.8 \times 10^{-15}$	$9.2 \times 10^5$
Latex sphere 0.05 $\mu\text{m}$	$4.8 \times 10^{-9}$	$9.5 \times 10^{-18}$	$2.3 \times 10^3$
MS2 (0.025 $\mu\text{m}$ )	$2.9 \times 10^{-9}$	$3.5 \times 10^{-18}$	$8.4 \times 10^2$

[30] The contact surface area of colloids can then be estimated from a flat surface with radius  $R_c$  as follows:

$$R_c = (R - D_0) \tan \theta \quad (12)$$

[31] The overall calculated capillary energy,  $W_{\text{cap}}$ , and  $D_0$  are reported in Table 2.  $D_0$  is of the order of nanometers (about 10% of the total diameter of the colloids used in these experiments.). Thus the colloids barely penetrate the AWI, which suggests that water is the main medium between the colloids attached at the AWI. Therefore the calculated energy barrier between colloids in the water and the energy barrier between colloids attached to the AWI should be similar. The values of  $W_{\text{cap}}$  are about 2–3 orders of magnitudes higher than the energy barrier calculated from DLVO theory shown in Figure 5a and 5b for the same types of colloids.

[32] The colloidal clusters observed in our experiments, especially those of 2 and 3  $\mu\text{m}$  latex colloids, could be generated either from incomplete dissolution of an air bubble, or from the coagulation of trapped colloids in the AWI, at the end of the dissolution process. Since the visual resolution limits us from observing the colloids at such fine scale, the preceding calculations could be used to estimate whether the colloids at the AWI can coagulate. After the colloids penetrate through the AWI, they remain attached to the AWI, and as the bubble shrinks, the colloids approach each other. In our system (air/water/colloids), the energy that holds the colloids at the AWI is predicted to be significantly larger than the energy barrier between the colloids. Therefore eventually the colloids will form clusters.

[33] Although the  $W_{\text{cap}}$  is small, in the range of  $10^{-18}$ – $10^{-14}$  J (Table 2), we did not observe the detachment of colloids from the AWI in our experiments. The detachment of colloids from the AWI was hypothesized by *Wan and Wilson* [1994b] and by *Corapcioglu and Choi* [1996]; to our knowledge, however, this has not been observed. For our system, lack of detachment of individual colloids could be due to weak interfacial shear stresses, given the slow fluid flow in our system; one would not expect strong shear stresses in porous media.

[34] It should be noted that we did not account for other non-DLVO forces in our analysis, such as repulsive hydration forces, which could be much stronger than the DLVO forces at small distances (nanoscale). Those forces could be monotonically attractive, monotonically repulsive, or oscillatory [*Israelachvili*, 1992]. Since the value of the Hamaker constant for our system is larger than  $10^{-21}$  J (Table 1), we do not expect the other non-DLVO forces to dominate the adhesion of two colloidal particles in our solution [*Israelachvili*, 1992]. Furthermore, the observation of clusters of colloids breaking off during the dissolution would be

an indicator that the cluster of colloids is a result of coagulation. Since the particles adhering to bubbles may promote bubble coalescence [*van der Zon et al.*, 2002], the breakoff of the cluster seems to be unlikely.

[35] The coagulation of colloids might occur in a natural groundwater system, following the same mechanisms observed in this study. After coagulation, we do not expect the colloidal clusters to break up. This would provide more filtration of colloids through the vadose zone than predicted from filtration of a single particle, due to the filtration of the clustered colloids. The type of colloids as well as the chemical and physical properties of the surrounding largely determine the stability of colloids in the natural system. Given that the ionic strength of the natural groundwater may be much higher than in our experimental setup, the energy barrier in natural systems would be lower, leading to coagulation, unless the colloids have much higher surface potential than observed here.

[36] In general, the results at the pore scale confirm the previous results obtained from column-scale experiments [*Corapcioglu and Choi*, 1996] that the AWI is a particle trap and particles will move along the column as the rewetting front advances. *Poletika et al.* [1995] also found more sorption of MS2 in unsaturated soil in the field-scale experiments than what they expected based on the laboratory sorption experiments. They hypothesized that the difference in field and laboratory sorption may be due to AWI processes in the unsaturated field experiments. The analytical models developed by *Sim and Chrysikopoulos* [1999] for adsorption and inactivation of virus in unsaturated porous media also suggested that virus removal is significantly enhanced due to the sorption of viruses onto the AWI, which is in general agreement with the results from the present study. The models can be modified to consider detachment of colloids during the imbibition stage, as the air bubbles dissolve.

#### 4. Conclusion

[37] According to our observations of colloids transport in unsaturated micromodel, we found that the particles attach strongly to the AWI and generally do not detach as long as there is an AWI. Once the air bubbles are near the end of the dissolution process, the colloids tend to form clusters, which are transported with the flow as colloidal clusters. These detached clusters may be trapped in an AWI down-gradient, or may be trapped in small pore throats, modifying the hydrodynamics of the system. When we compared the energy barrier between particles, following DLVO theory, to the forces that hold the colloids at the AWI (mainly capillary forces), the calculation indicates that the attraction energy of the colloids at the AWI is larger than the energy barrier between the colloids. Therefore it is quite likely that the cluster of colloids is formed by the colloids attached at the AWI as they move closer at the end of the bubble dissolution process and pass the energy barrier. We do not expect the colloids in our system to coagulate in solution; however, this might be quite different for other colloids or under different aqueous matrix conditions. Coagulation at the AWI may be a significant mechanism for colloid transport through the vadose zone, increasing their overall filtration. Just as important, colloids trapped in the AWI might be quite mobile when the air bubbles are

transported at the end of the dissolution process, resulting in increased breakthrough. These pore-scale mechanisms are likely to play a significant role in the macroscopic transport of colloids in unsaturated porous media.

[38] **Acknowledgments.** The authors wish to acknowledge partial funding from U.S. EPA Exploratory Research Grant R826268 and U.S. EPA grant R827133, as well as from the University of California Water Resources Center and the UCSB Academic Senate. The authors also wish to thank J. N. Israelachvili for intellectual contribution to this work, as well as the detailed and thoughtful comments from the two anonymous reviewers.

## References

- Abdel-Fattah, A. I., and M. S. El-Genk, Sorption of hydrophobic, negatively charged microspheres onto stagnant air/water interface, *J. Colloid Interface Sci.*, 202, 417–429, 1998a.
- Abdel-Fattah, A. I., and M. S. El-Genk, On colloidal particle sorption onto a stagnant air-water interface, *Adv. Colloid Interface Sci.*, 78, 237–266, 1998b.
- Balch, W. M., J. Vaughn, J. Novotny, D. T. Drapeau, R. Vaillancourt, J. Lapierre, and A. Ashe, Light scattering by viral suspensions, *Limnol. Oceanogr.*, 45, 492–498, 2000.
- Bales, R. C., C. P. Gerba, G. H. Grondin, and S. L. Jensen, Bacteriophage transport in sandy soil and fractured tuff, *Appl. Environ. Microbiol.*, 55, 2061–2067, 1989.
- Bradford, S. A., S. R. Yates, M. Bettahar, and J. Simunek, Physical factors affecting the transport and fate of colloids in saturated porous media, *Water Resour. Res.*, 38(12), 1327, doi:10.1029/2002WR001340, 2002.
- Chrysikopoulos, C. V., and Y. Sim, One-dimensional virus transport in homogeneous porous media with time-dependent distribution coefficient, *J. Hydrol.*, 185(1–4), 199–219, 1996.
- Corapcioglu, M. Y., and H. Choi, Modeling colloid transport in unsaturated porous media and validation with laboratory column data, *Water Resour. Res.*, 32, 3437–3449, 1996.
- Corapcioglu, M. Y., and S. Y. Jiang, Colloid-facilitated groundwater contaminant transport, *Water Resour. Res.*, 29, 2215–2226, 1993.
- Ducker, W. A., Z. Xu, and J. N. Israelachvili, Measurements of hydrophobic and DLVO forces in bubble-surface interactions in aqueous solutions, *Langmuir*, 10, 3279–3289, 1994.
- Dufrène, Y. F., A. van der Wal, W. Norde, and P. G. Rouxhet, X-ray photoelectron spectroscopy analysis of whole cell and isolated cell walls of gram-positive BACTERIA: Comparison with biochemical analysis, *J. Bacteriol.*, 179, 1023–1028, 1997.
- Gregory, J., Interaction of unequal double layers at constant charge, *J. Colloid Interface Sci.*, 51, 44–51, 1975.
- Hennes, K. P., C. A. Suttle, and A. M. Chan, Fluorescently labeled virus probes show that natural virus populations can control structure of marine microbial communities, *Appl. Environ. Microbiol.*, 61, 3623–3627, 1995.
- Hiemenz, P. C., and R. Rajagopalan, *Principles of Colloid and Surface Chemistry*, 3rd ed., Marcel Dekker, New York, 1997.
- Holden, P. A., Biofilms in unsaturated environments, *Methods Enzymol.*, 337, 125–143, 2001.
- Israelachvili, J. N., *Intermolecular and Surface Forces*, 2nd ed., Academic, San Diego, Calif., 1992.
- Jin, Y., and M. Flury, Fate and transport of viruses in porous media, *Adv. Agron.*, 77, 39–102, 2002.
- Keller, A. A., M. J. Blunt, and P. V. Roberts, Micromodel observation of the role of oil layers in three-phase flow, *Transp. Porous Media*, 26, 277–297, 1997.
- Lance, J. P., and C. P. Gerba, Virus movement in soil during saturated and unsaturated flow, *Appl. Environ. Microbiol.*, 47, 335–337, 1984.
- Macler, B. A., and J. C. Merkle, Current knowledge on groundwater microbial pathogens and their control, *Hydrogeol. J.*, 8, 24–40, 2000.
- McCarthy, J. F., and J. M. Zachara, Subsurface transport of contaminants—Mobile colloids in the subsurface environment may alter the transport of contaminants, *Environ. Sci. Technol.*, 23, 496–502, 1989.
- McDowellboyer, L. M., J. R. Hunt, and N. Sitar, Particle-transport through porous media, *Water Resour. Res.*, 22, 1901–1921, 1986.
- Parsegian, V. A., Spectroscopic parameters for computation of van der Waals forces, *J. Colloid Interface Sci.*, 81, 285–289, 1981.
- Penrod, S. L., T. M. Olson, and S. B. Grant, Deposition kinetics of two viruses in packed beds of quartz granular media, *Langmuir*, 12, 5576–5587, 1996.
- Poletika, N. N., W. A. Jury, and M. V. Yates, Transport of bromide, simazine, and MS2 coliphage in a lysimeter containing undisturbed, unsaturated soil, *Water Resour. Res.*, 31, 801–810, 1995.
- Powelson, D. K., J. R. Simpson, and C. P. Gerba, Virus transport and survival in saturated and unsaturated flow through soil columns, *J. Environ. Qual.*, 19, 396–401, 1990.
- Reddy, V. S., H. A. Giesing, R. T. Morton, A. Kumar, C. B. Post, I. Charles, L. Crooks, and J. E. Johnson, Energetics of quasiequivalence: Computational analysis of protein-protein interactions in icosahedral viruses, *Bio-phys. J.*, 74, 546–558, 1998.
- Rehmann, L. L. C., C. Welty, and R. W. Harvey, Stochastic analysis of virus transport in aquifers, *Water Resour. Res.*, 35, 1987–2006, 1999.
- Schijven, J. F., and S. M. Hassanizadeh, Removal of viruses by soil passage: Overview of modeling, processes, and parameters, *Crit. Rev. Environ. Sci. Technol.*, 30(1), 49–127, 2000.
- Shaw, D. J., *Introduction to Colloid and Surface Chemistry*, 4th ed., Butterworth-Heinemann, Woburn, Mass., 1992.
- Sim, Y., and C. V. Chrysikopoulos, Analytical models for one-dimensional virus transport in saturated porous media, *Water Resour. Res.*, 32, 1473, 1996.
- Sim, Y., and C. V. Chrysikopoulos, Analytical models for virus adsorption and inactivation in unsaturated porous media, *Colloids Surf. Physico-chem. Eng. Aspects*, 155, 189–197, 1999.
- Sim, Y., and C. V. Chrysikopoulos, Virus transport in unsaturated porous media, *Water Resour. Res.*, 36, 173–179, 2000.
- Sirivithayapakorn, S., and A. Keller, Transport of colloids in saturated porous media: A pore-scale observation of the size exclusion effect and colloid acceleration, *Water Resour. Res.*, 39(4), 1109, doi:10.1029/2002WR001583, 2003.
- Small, H., Hydrodynamic chromatography: A technique for size analysis of colloidal particles, *J. Colloid Interface Sci.*, 48, 147–161, 1974.
- Tchaliovskia, S., P. Herder, R. Pugh, P. Stenius, and J. C. Eriksson, Studies of the contact interaction between an air bubble and a mica surface submerged in dodecylammonium chloride solution, *Langmuir*, 6, 1535–1543, 1990.
- Usui, S., H. Sasaki, and H. Matsukawa, The dependence of zeta potential on bubble size as determined by Dom effect, *J. Colloid Interface Sci.*, 81, 80–84, 1981.
- van der Zon, M., P. J. Hamersma, E. K. Poels, and A. Blik, Coalescence of freely moving bubbles in water by the action of suspended hydrophobic particles, *Chem. Eng. Sci.*, 57, 4845–4853, 2002.
- Wan, J. M., and J. L. Wilson, Colloid transport in unsaturated porous media, *Water Resour. Res.*, 30, 857–864, 1994a.
- Wan, J. M., and J. L. Wilson, Visualization of the role of the gas-water interface on the fate and transport of colloids in porous media, *Water Resour. Res.*, 30, 11–23, 1994b.
- Wan, J., J. L. Wilson, and T. L. Kieft, Influence of the gas-water interface on transport of microorganisms through unsaturated porous media, *Appl. Environ. Microbiol.*, 60, 509–516, 1994.
- Yates, M. V., and Y. Ouyang, VIRTUS, a model of virus transport in unsaturated soils, *Appl. Environ. Microbiol.*, 58, 1609–1616, 1992.

A. Keller and S. Sirivithayapakorn, Bren School of Environmental Science and Management, University of California, Santa Barbara, Santa Barbara, CA 93106, USA. (sanya@bren.ucsb.edu)